SUMMARY AND CONCLUSIONS

6.1. Summary

During the past few decades, a large number of hydrazones, semicarbazones and isatin derivatives have been documented as potential bioactive compounds.

In the present work, we attempted to identify new MAO and AChE inhibitors and multi-target-directed ligands (MTDLs) with dual MAO and AChE inhibitory properties. For this, we designed and synthesized four different series of compounds namely 2-amino-6-nitrobenzothiazole derived extended hydrazones (**BTA-1** to **BTA-30**) incorporated with a flexible amino methyl carbonyl hydrazino linker (–NH–CH_2–CO–NH–N=C<), 2-amino-5-nitrothiazole derived semicarbazones (**NTA-1** to **NTA-18**), 3,4-(methylenedioxy)aniline derived semicarbazones (**MDA-1** to **MDA-14**) possessing a flexible semicarbazino linker (–NH–CO–NH–N=C<) and rigid 3-hydroxy-3-substituted oxindole analogues of isatin with a short, less flexible acetyl (–CO–CH_2–) linker (**HPO-1** to **HPO-14**) based on the MTDL approach and evaluated their bioactive potential in virtual and physical environments through virtual molecular docking and physical enzymatic screening assays (*in-vitro* MAO and AChE inhibition assay) respectively.

The compounds were also evaluated for other neurological properties such as *in-vivo* antidepressant activity, anxiolytic activity, sedative-hypnotic activity and neurotoxicity. In addition some of the selected compounds were screened for the antioxidant activity using DPPH radical scavenging assay. The most potent compounds were also investigated for their effect on liver function and the hepatotoxicity was assessed by histopathological studies. *In-silico* molecular property analysis and ADMET prediction studies were also carried out to predict the drug-likeness and pharmacokinetic profile of the compounds.

From the preliminary *in-vitro* MAO and AChE inhibition studies, we identified one lead compound from each series (**Figure 6.1.**) possessing dual inhibition potential against both the enzymes with minimal or no toxicity.

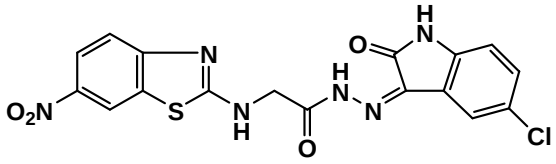

BTA-29

MAO-A IC_{50} = 1.38 ± 0.002 μM
MAO-B IC_{50} = 0.0018 ± 0.0003 μM
AChE IC_{50} = 0.035 ± 0.005 μM
Mildly neurotoxic (25% at 0.5 h)
Non-hepatotoxic

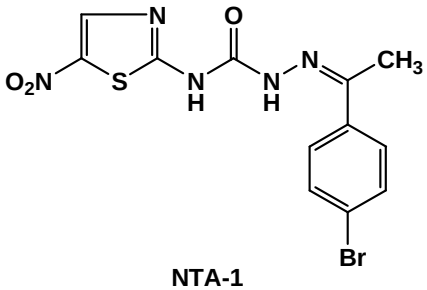

NTA-1

MAO-A IC_{50} = 70.19 ± 0.045 μM
MAO-B IC_{50} = 0.212 ± 0.004 μM
AChE IC_{50} = 0.340 ± 0.007 μM
Mildly neurotoxic (25% at 0.5 h)
Non-hepatotoxic

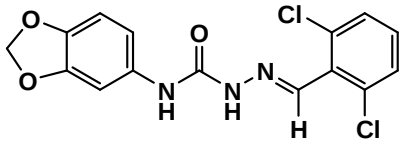

MDA-7

MAO-A IC_{50} = 4.52 ± 0.032 μM
MAO-B IC_{50} = 0.059 ± 0.002 μM
AChE IC_{50} = 0.0087 ± 0.0002 μM
Non-neurotoxic
Non-hepatotoxic

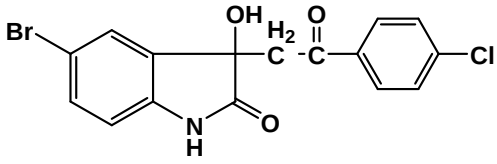

HPO-9

MAO-A IC_{50} = 0.071 ± 0.003 μM
MAO-B IC_{50} = 0.235 ± 0.0003 μM
AChE IC_{50} = 0.967 ± 0.004 μM
Non-neurotoxic
Non-hepatotoxic

Figure 6.1. Structures of identified lead compounds possessing dual inhibition potential against MAO and AChE

6.1.1. Summary of MAO inhibition studies

Most of the compounds belonging to BTA, NTA and MDA series were found to be more selective towards MAO-B isozyme than MAO-A. However, the compounds of HPO series were found to be more potent and selective towards MAO-A.

6.1.1.1. Comparison of lead MAO-B inhibitors across the series (extended hydrazones and semicarbazones)

The lead MAO-B inhibitors belonging to BTA (**BTA-29**), NTA (**NTA-1**) and MDA (**MDA-7**) series incorporated with the flexible linker were compared with a semicarbazone-based lead MAO-B inhibitor **SBTZ-18 (**IC_{50} = 0.004 μM) identified earlier in our laboratory (**Figure 6.2.**).

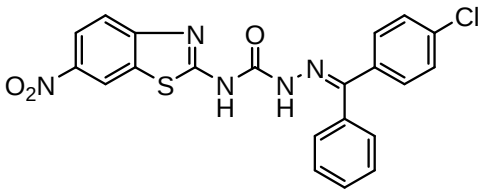

Lead MAO-B inhibitor from earlier study (SBTZ-18)
IC_{50} : 0.004 μM (Expt.)
K_i : 1.55 μM (Comp.)

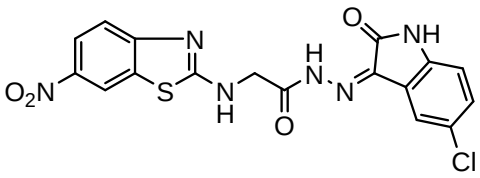

Lead MAO-B inhibitor of BTA series (BTA-29)
IC_{50} : 0.0018 μM (Expt.)
K_i : 1.97 μM (Comp.)

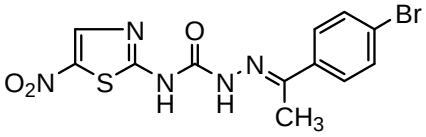

Lead MAO-B inhibitor of NTA series (NTA-1)
IC_{50} : 0.212 μM (Expt.)
K_i : 13.84 μM (Comp.)

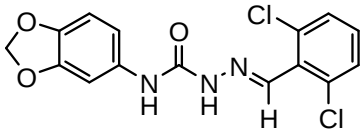

Lead MAO-B inhibitor of MDA series (MDA-7)
IC_{50} : 0.059 μM (Expt.)
K_i : 1.92 μM (Comp.)

Figure 6.2. Lead MAO-B inhibitors

On comparing the hydrazone lead **BTA-29** to **SBTZ-18**, it was observed that the incorporation of methylene spacer to the semicarbazone linker increased the activity (~2.22 folds to that of **SBTZ-18**) and selectivity towards MAO-B.

The docking simulations have shown that the selectivity of inhibitor **BTA-29** for MAO-B is likely due to the pose obtained for **BTA-29** within the active site of hMAO-B showing preference for the ligand to be placed in a deeper region well occupying both the entrance and the substrate cavities, resulting in an energetically favourable complex.

Further, **BTA-29** established better interactions with the MAO-B active site compared to that of MAO-A indicating that **BTA-29** interacted more tightly with MAO-B. The reason behind this may be the variation in the geometry adopted by **BTA-29** which permitted better accommodation within the active site of MAO-B than MAO-A.

Comparison of virtual binding modes of the lead MAO-B inhibitors was also made and is illustrated in **Figure 6.3.** It was observed that the synthesized hydrazone lead **BTA-29** and the semicarbazone leads **NTA-1** and **MDA-7** occupied the active site of MAO-B with the binding pose similar to that of the **SBTZ-18** (**Figure 6.3. (A)**).

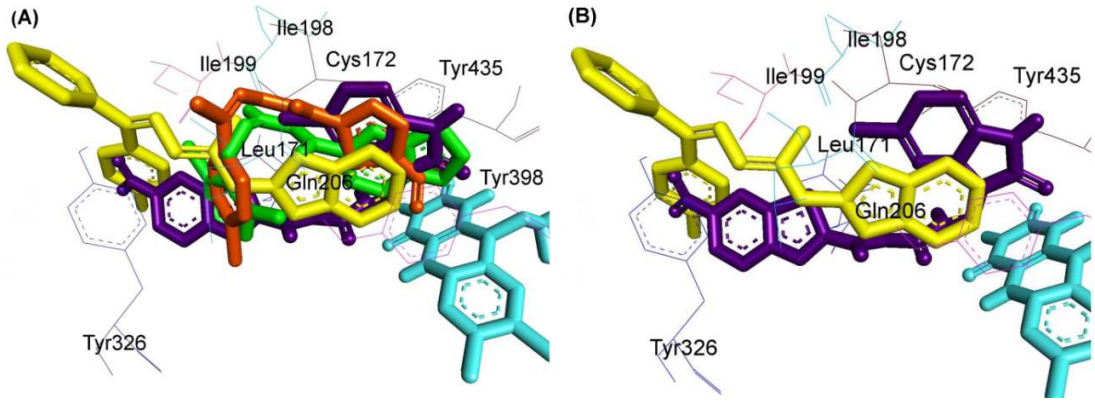

Figure 6.3. Comparison of binding modes of (A) Hydrazone lead **BTA-29** (violet) and semicarbazone leads **NTA-1** (orange), **MDA-7** (green) and **SBTZ-18** (yellow) (B) Hydrazone lead **BTA-29** and semicarbazone lead **SBTZ-18**

Based on the potential MAO-B inhibitory activity displayed by these lead inhibitors, it can be concluded that

- A large hydrophobic heterocyclic ring (A) is essential for binding with the substrate cavity of MAO-B.
- Another hydrophobic aryl ring (B) with electronegative substituents is crucial for effective binding and stabilization in the entrance cavity space of MAO-B.
- A flexible linker preferably with H-bond acceptor and H-bond donor groups is essential for guiding optimal orientation of both the hydrophobic aryl residues in their respective binding pockets within the active site of MAO-B.
- Distance between the aryl binding sites (A and B) should be 9.0 – 10.5 Angstroms.

Accordingly, we propose a three site PCP model (**Figure 6.4.**) for MAO-B inhibitors which can be used for the future design of MAO-B inhibitors.

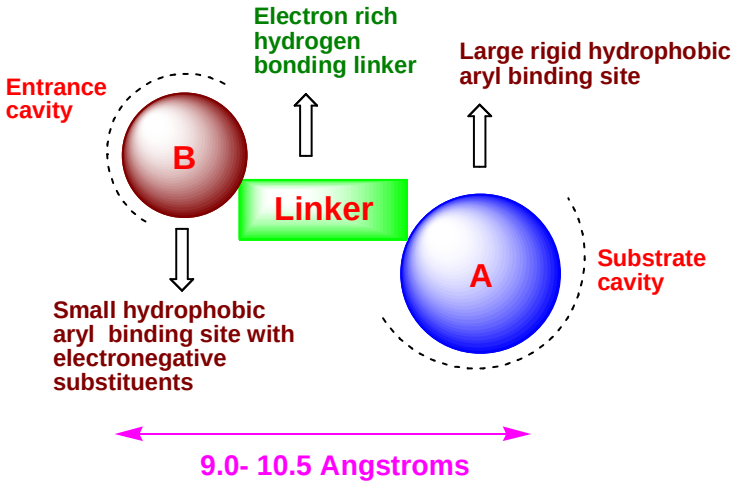

Figure 6.4. Proposed three site PCP model for MAO-B inhibitors showing essential pharmacophoric features

6.1.1.2. Comparison of lead MAO-A inhibitors across the series

Most of the compounds of 3-hydroxy-3-substituted oxindole analogues of isatin (HPO series) were found to be more potent and selective towards MAO-A isozyme. The lead MAO-A inhibitor obtained was **HPO-9** (**Figure 6.5.**). The preferential MAO-A selectivity of these analogues could be ascribed to their molecular shape and the rigidity imparted by isatin moiety, enabling a better accommodation into the MAO-A binding site, which is wider and less flat than that of MAO-B.

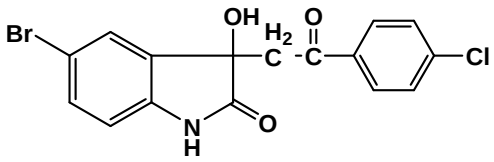

Lead MAO-A inhibitor: HPO-9

IC_{50} = 0.071 ± 0.003 µM

Figure 6.5. Lead MAO-A inhibitor

Based on the potential MAO-A inhibitory activity displayed by **HPO** series, it can be concluded that

- Presence of two aryl binding sites are essential, out of which one should be a large rigid moiety with a H-bond acceptor and a H-bond donor group for optimal binding to the active site of MAO-A.

- ❖ A less flexible, shorter linker (compared to **BTA**, **NTA** and **MDA** series) is essential to guide both the aryl binding moieties inside the cavity space.
- ❖ Distance between the two aryl binding sites should be 7.0 – 8.0 Angstroms.

The proposed PCP model for MAO-A inhibitors showing the essential pharmacophoric features is illustrated in **Figure 6.6.**

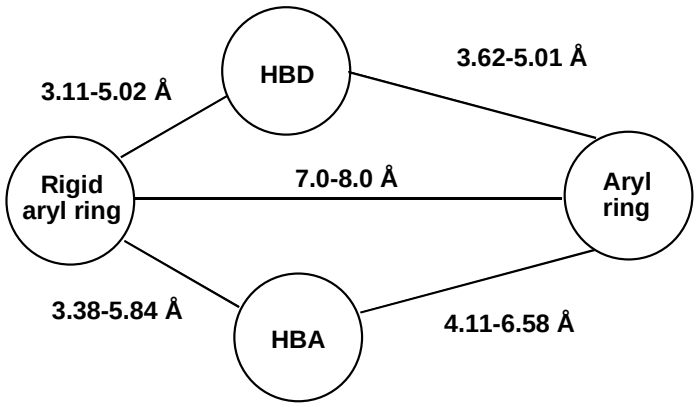

Figure 6.6. Proposed PCP model for MAO-A inhibitors showing essential pharmacophoric features with distance constraints

6.1.2. Summary of AChE inhibition studies

Most of the compounds belonging to BTA, NTA and MDA series were found to be potent inhibitors of AChE enzyme. The lead AChE inhibitors obtained from our study are **BTA-29**, **NTA-18**, **MDA-7** and **HPO-9** (**Figure 6.7.**).

Comparison of virtual binding modes of the lead AChE inhibitors is illustrated in **Figure 6.8.** It was observed that the synthesized hydrazone lead **BTA-29** and the semicarbazone leads **NTA-18** and **MDA-7** and 3-hydroxy-3-substituted oxindole analogue of isatin **HPO-9** occupied the active site gorge of AChE with the hydrophobic aryl rings simultaneously occupying both the catalytic anionic site (CAS) and peripheral anionic site (PAS) with the hydrazino and semicarbazino linkers occupying the middle of the gorge between CAS and PAS.

The higher potency of **MDA-7** may be because of the linear conformation of **MDA-7** which allows it to span both CAS and PAS cavities of AChE thereby contributing to its superior binding towards AChE. Whereas the other lead inhibitors (**BTA-29**, **NTA-18**

and **HPO-9**) adopted a non-linear conformation which eventually resulted in decreased potency and affinity.

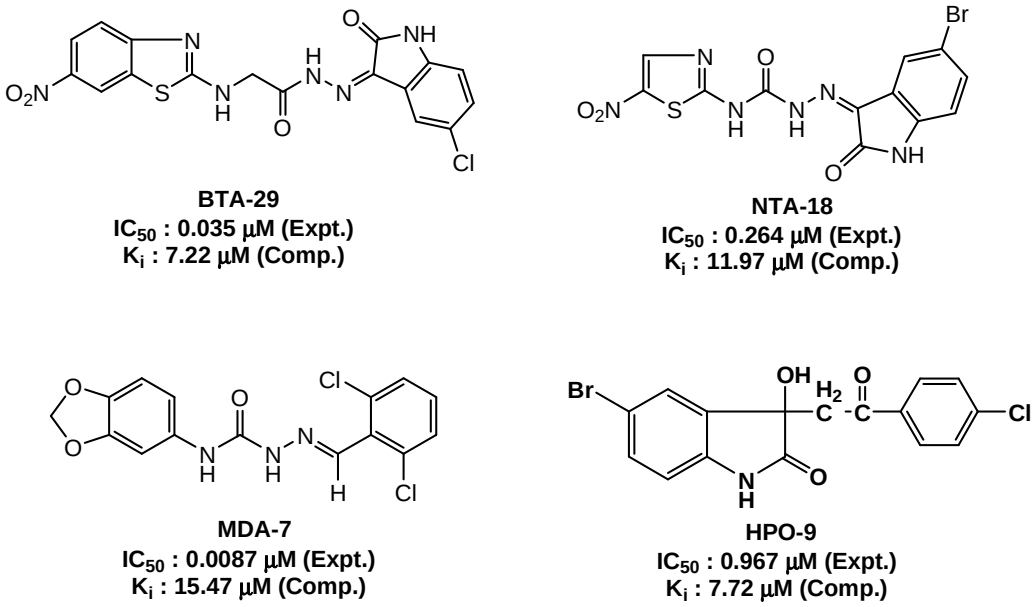

Figure 6.7. Lead AChE inhibitors

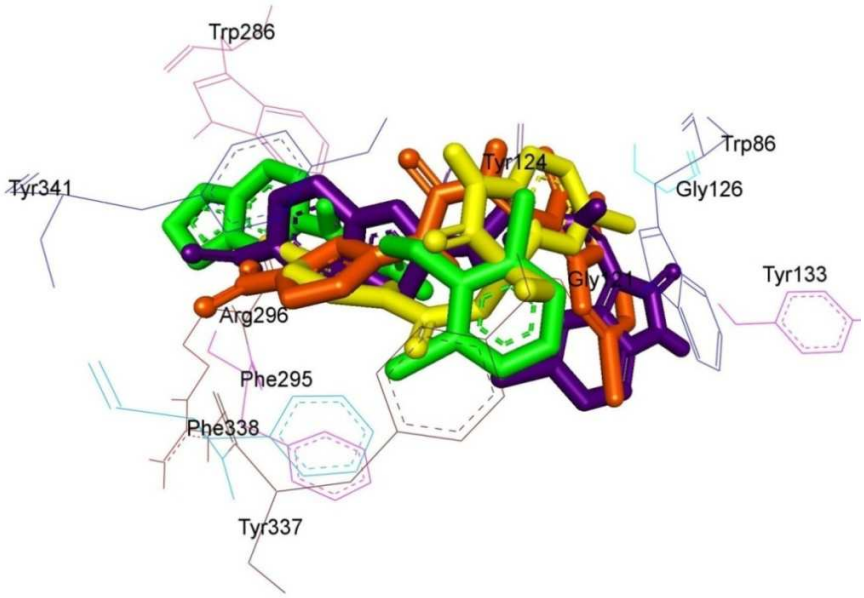

Figure 6.8. Comparison of binding modes of lead AChE inhibitors **BTA-29** (violet), **NTA-18** (orange), **MDA-7** (linear pose, green) and **HPO-9** (yellow)

Based on the potential AChE inhibitory activity displayed by the lead inhibitors, it can be concluded that

- ❖ Two hydrophobic heteroaryl/aryl rings are crucial for the effective binding and stabilization within the CAS and PAS of AChE.
- ❖ Presence of flexible linker preferably with a H-bond acceptor, a H-bond donor and an electron donor group is essential for guiding optimal orientation of both the hydrophobic aryl residues within the active site gorge of AChE.

The proposed 2D binding site model for AChE inhibitors showing the essential pharmacophoric features is illustrated in **Figure 6.9.**

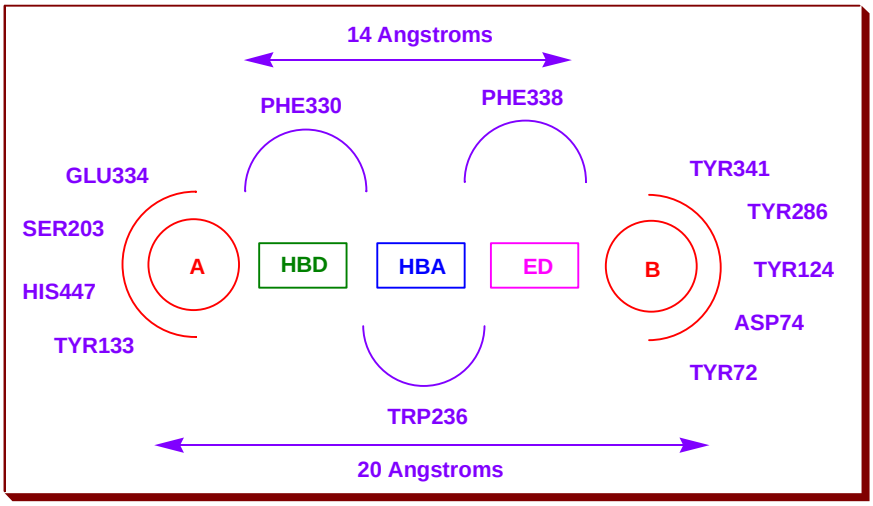

Figure 6.9. Proposed 2D binding site model for AChE inhibitors showing essential pharmacophoric features [A, B – Hydrophobic domains; HBD – H-bond donor group; HBA – H-bond acceptor group; ED – Electron donor group]

6.1.3. Summary of behavioural studies

To assess the behavioural activity profile viz. antidepressant, anxiolytic and sedative-hypnotic activities, of the synthesized compounds, standard animal models were utilized namely Porsolt's forced swim test, elevated plus maze test and pentobarbitone potentiation test respectively.

Antidepressant activity

All the synthesized compounds were evaluated for antidepressant activity using Porsolt's forced swim test. Few compounds viz. **BTA-3**, **BTA-15**, **BTA-17**, **BTA-29**, **NTA-9**,

NTA-18, **MDA-7** and **MDA-9** were found to be more active than the reference standard citalopram, thereby indicating that these compounds produce no CNS depression.

Anxiolytic activity

All the synthesized compounds were screened for anxiolytic activity using elevated plus maze apparatus. Most of the compounds viz. **BTA-3**, **BTA-22** to **BTA-24**, **BTA-26**, **BTA-28** to **BTA-30**, **NTA-1** to **NTA-7**, **NTA-9**, **NTA-12** to **NTA-18**, **MDA-2**, **MDA-5** to **MDA-7**, **MDA-9**, **MDA-13**, **HPO-3**, **HPO-6**, **HPO-7** and **HPO-9** exhibited significantly greater anxiolytic activity than the reference standard diazepam while **BTA-12** and **BTA-14** expressed potency equivalent to diazepam.

Sedative-hypnotic activity

All the synthesized compounds were evaluated for the sedative-hypnotic activity using Pentobarbitone potentiation test. Majority of the compounds belonging to **BTA**, **NTA**, **MDA** and **HPO** series lack sedative effect with the exception of compounds **BTA-4** to **BTA-6**, **BTA-9**, **BTA-12**, **BTA-22**, **BTA-29**, **NTA-1**, **NTA-5** to **NTA-7**, **NTA-16**, **NTA-18**, **HPO-6** and **HPO-8** which were found to potentiate pentobarbitone induced narcosis.

6.1.4. Summary of neurotoxicity screening

Selected compounds of **BTA**, **NTA**, **MDA** and **HPO** series were screened for neurotoxicity by rotarod apparatus. Among the tested compounds, all were found to be non-neurotoxic except compounds **BTA-3**, **BTA-29**, **BTA-30**, **NTA-18**, **MDA-14** which were found to be mildly neurotoxic; and **NTA-6**, **MDA-12** and **HPO-12** which were found to be moderately neurotoxic compared to reference standard phenytoin.

6.1.5. Summary of antioxidant activity studies

Selected compounds belonging to all four series were tested for their antioxidant potential by *in vitro* DPPH radical scavenging assay. Some compounds viz. **BTA-3** (61.62%), **BTA-10** (63.65%), **BTA-26** (62.25%), **BTA-28** (63.54%), **BTA-29** (64.74%), **BTA-30** (63.13%), **NTA-18** (65.65%), **MDA-5** (62.59%), **MDA-6** (63.27%), **MDA-7** (65.98%), **MDA-9** (64.37%), **HPO-7** (62.03%), **HPO-9** (63.76%) and **HPO-10** (61.35%) exhibited antioxidant activity (expressed as % inhibition) higher than the reference antioxidant ascorbic acid (61.24%).

6.1.6. Summary of liver toxicity studies

Hepatotoxicity studies of the lead compounds from each series viz. **BTA-29**, **NTA-1**, **NTA-18**, **MDA-7**, **MDA-9**, **HPO-7** and **HPO-9** were accomplished to check the magnitude of liver toxicity. The results indicated that five compounds **BTA-29**, **NTA-1**, **MDA-7**, **MDA-9** and **HPO-7** were non-hepatotoxic while remaining compounds **NTA-18** and **HPO-9** were found to show mild to moderate hepatotoxicity.

6.2. Conclusions

As summarized above, our present work entitled "Rational design, synthesis, *in-silico* screening and evaluation of some heterocyclic compounds as neurotherapeutic agents" yielded some lead MAO/AChE and dual inhibitors with interesting activity profile.

BTA-29 (N'-(5-chloro-2-oxoindolin-3-ylidene)-2-(6-nitrobenzothiazol-2-ylamino)aceto-hydrazide) and **MDA-7** (1-(2,6-dichlorobenzylidene)-4-(benzo[1,3]dioxol-5-yl)semicarbazide) have emerged as the most promising dual acting lead compounds (**Figure 6.10.**) which warrants further clinical development as neurotherapeutic agents.

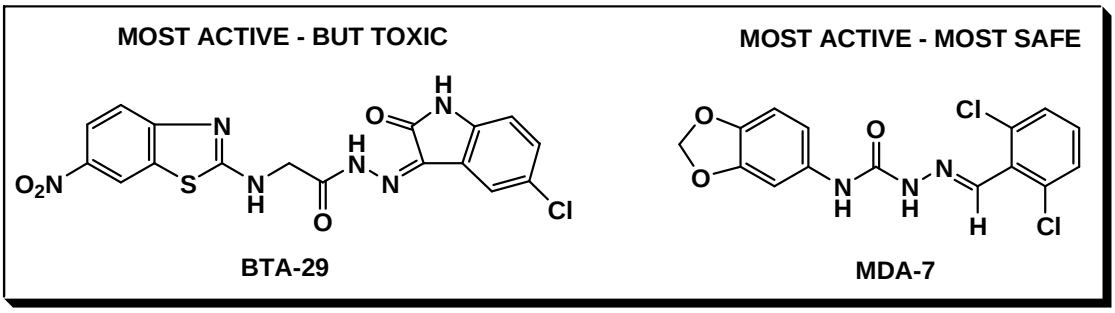

Figure 6.10. Dual acting lead MAO/AChE inhibitors

The comprehensive binding site and pharmacophore models proposed in this study can be used for the future design of novel potent and selective MAO/AChE inhibitors.

The lead MTDLs identified from the study (**BTA-29** and **MDA-7**) exhibited a pharmacological profile almost identical to the investigational drug (MTDL) Ladostigil. **BTA-29** and **MDA-7** exhibited better MAO-B and AChE inhibitory activity respectively than the marketed drugs rasagiline and donepezil. The lead MTDLs were found to be a dual brain acetylcholine and MAO-A/B inhibitor, intended for the treatment of dementia

co-morbid with depression and anxiety without causing any sedation. Furthermore, both the leads demonstrated antioxidant activity *in-vitro* thereby indicating its role in preventing oxidative stress. Additionally, the leads exhibited *in-vivo* neuroprotection in neurotoxicity rat model and were found to be non-hepatotoxic. Thus, the research work provided the pre-clinical scientific evidence for the therapeutic potential of these lead MTDLs in treating neurodegenerative diseases.

Further studies like

(i) Co-crystallization studies of the enzyme-lead inhibitor complex (for both MAO-A/-B & AChE)

(ii) Lead optimization studies to reduce the toxicity and retain or further enhance the potency

(iii) Experimental pharmacokinetic studies, etc.

of these lead compounds are essential to develop them as potential neurotherapeutic candidates for the treatment of NDDs.